



Ultrafast MRI in BI-RADS 4 Masses: The Fast Lane to Clarity

Veenu Singla¹ Joseph Johnson¹ Dollphy Garg¹ Tulika Singh¹ Nidhi Prabhakar¹ Amanjit Bal² Siddhant Khare³

¹Department of Radiodiagnosis and Imaging, Postgraduate Institute of Medical Education and Research, Chandigarh, India

²Department of Histopathology, Postgraduate Institute of Medical Education and Research, Chandigarh, India

³Department of General Surgery, Postgraduate Institute of Medical Education and Research, Chandigarh, India

Address for correspondence Veenu Singla, MD, Department of Radiodiagnosis and Imaging, Postgraduate Institute of Medical Education and Research, Chandigarh 160012, India (e-mail: veenupgi@gmail.com).

Indian J Radiol Imaging 2026;36:192–201.

Abstract

Objective This study aims to evaluate the diagnostic accuracy of ultrafast magnetic resonance imaging (UF-MRI)-derived kinetic parameters in differentiating benign from malignant BI-RADS (Breast Imaging-Reporting and Data System) 4 breast masses. It also compares the performance of UF-MRI with standard dynamic contrast-enhanced MRI (DCE-MRI) to determine its impact on clinical decision-making and overall diagnostic accuracy.

Materials and Methods This cross-sectional observational study included patients with BI-RADS 4 breast masses who underwent UF-MRI from January to December 2024. UF-MRI was acquired continuously over a brief period, capturing kinetic parameters including time to enhancement (TTE), arterial-venous interval (AVI), and maximum slope (MS), in addition to standard DCE-MRI. Two radiologists with more than 10 years of experience in breast radiology independently evaluated the results from standard DCE-MRI and UF-MRI. Statistical analysis assessed the correlation between UF-MRI parameters, standard DCE-MRI, and final histopathology.

Results A total of 31 breast masses from 29 patients (mean age: 45.3 ± 10.9 years) were evaluated, with 16 malignant and 15 benign masses confirmed on histopathology. UF-MRI parameters TTE and AVI demonstrated a strong correlation with malignancy (Cramer's V: 0.81 and 0.87, $p < 0.001$) while MS (Cramer's V: 0.50) showed moderate association. AVI had the highest specificity (86.7%), followed by TTE (80%) and MS (66.7%) when compared with standard DCE-MRI kinetic curves that showed significantly lower specificity (40%). The combined accuracy of TTE + AVI + MS was 93.5%, with an area under curve of 0.969. UF-MRI showed a high sensitivity and specificity of 100 and 87%, respectively.

Conclusion UF-MRI offers a fast and accurate approach for distinguishing benign from malignant BI-RADS 4 lesions, with TTE and AVI emerging as highly reliable diagnostic markers. It addresses the limitations of standard DCE-MRI by providing early

Keywords

- ▶ ultrafast
- ▶ breast MRI
- ▶ dynamic contrast-enhanced MRI
- ▶ wash-in curve
- ▶ BI-RADS 4
- ▶ kinetic

article published online
June 11, 2025

DOI <https://doi.org/10.1055/s-0045-1809444>.
ISSN 0971-3026.

© 2025. Indian Radiological Association. All rights reserved.
This is an open access article published by Thieme under the terms of the Creative Commons Attribution-NonDerivative-NonCommercial-License, permitting copying and reproduction so long as the original work is given appropriate credit. Contents may not be used for commercial purposes, or adapted, remixed, transformed or built upon. (<https://creativecommons.org/licenses/by-nc-nd/4.0/>)
Thieme Medical and Scientific Publishers Pvt. Ltd., A-12, 2nd Floor, Sector 2, Noida-201301 UP, India

contrast wash-in dynamic data with shorter acquisition times and higher specificity. Integrating UF-MRI kinetic parameters with morphological characteristics such as shape and margins can significantly enhance diagnostic precision, especially in patients with dense breasts and multiple masses, thereby minimizing the need for unnecessary biopsies.

Introduction

Breast cancer remains a major global health concern, with its incidence rising alarmingly and ranking among the leading causes of cancer-related deaths in women.¹ While mammography is the primary screening tool, it has notable limitations, including interval cancers, a restricted field of view, and reduced sensitivity in dense breast tissue, particularly in younger women.^{1,2} Ultrasound serves as a valuable adjunct but is highly operator-dependent, leading to significant inter- and intra-observer variability. These inconsistencies are further compounded by the inherent challenge of BI-RADS (Breast Imaging-Reporting and Data System) 4 classification, where the estimated malignancy risk varies widely from 3 to 94%.³ The broad spectrum of risk assessment reduces specificity and positive predictive value (PPV), increasing reliance on invasive procedures. However, in cases of multiple small breast masses, sampling each mass often becomes impractical.

With the increasing adoption of breast-conserving surgery, accurate preoperative assessment of disease extent has become crucial for optimizing surgical planning and improving patient outcomes. Magnetic resonance imaging (MRI), with its superior sensitivity and ability to provide both anatomical and functional imaging, helps in characterizing and detecting multifocal and multicentric lesions more efficiently.³⁻⁸ It preferentially detects invasive, high-grade cancers at earlier stages, often before axillary nodal involvement, leading to significant survival benefits.^{9,10} Compared with mammography, it demonstrates higher sensitivity and lower interval cancer rates, reinforcing its potential as a more effective screening tool. However, its widespread implementation remains limited due to high costs, restricted accessibility, and lengthy acquisition times, which impact workflow efficiency. To overcome these limitations, techniques such as abbreviated and ultrafast MRI (UF-MRI) have been introduced to improve accessibility and cost-efficiency.¹¹

Abbreviated MRI protocols have significantly reduced scan and interpretation times; however, the omission of dynamic kinetic information has led to lower specificity and increased recall rates.¹¹ UF-MRI has emerged as a transformative solution, reintroducing dynamic imaging while maintaining reasonable spatial resolution and short scan time. In standard dynamic contrast-enhanced MRI (DCE-MRI), temporal resolution typically exceeds 60 seconds, leading to the loss of critical early-phase kinetic information. A standard diagnostic protocol includes a pre-contrast T1-weighted image, followed by a brief 1-minute

delay after contrast administration to allow uniform tissue distribution. UF-MRI enables rapid image acquisition at multiple time points during the early phase of contrast by achieving high temporal resolution and preserving critical dynamic information. It can be seamlessly integrated into the routine diagnostic workflow during the initial delay without increasing acquisition time. Advances in acquisition techniques, such as view sharing, compressed sensing, and parallel imaging, have made this significant advancement possible.¹²⁻¹⁵ The UF-MRI acquisition begins 10 seconds postcontrast injection and continues for about an average of 66 seconds, after which the standard dynamic imaging phase commences and continues for a total scan duration of 5 minutes.

UF-MRI enhances the detection of hypervascularity, a key feature of malignancy, by analyzing the time of arrival of contrast from the aorta. Malignant lesions typically exhibit faster contrast inflow compared with benign masses and background parenchymal enhancement (BPE), making UF-MRI particularly valuable for younger women with moderate to marked BPE, where conventional imaging may be less reliable.¹⁶ In standard DCE-MRI, malignant breast tumors generally show rapid contrast uptake followed by washout in the delayed phase, making kinetic curve analysis an important complement to morphologic assessment. To improve early detection, UF-MRI introduces advanced kinetic parameters such as maximum slope (MS), time-to-enhancement (TTE), and arterial venous interval (AVI), which provide valuable insights into early contrast dynamics.^{17,18}

This is a feasibility study to evaluate the efficacy of UF-MRI in characterizing BI-RADS 4 masses. To the best of our knowledge, this is the first study assessing the clinical applicability of UF-MRI in the Indian setting.

Materials and Methods

This cross-sectional observational study was performed in a tertiary care center from January 2024 to December 2024. Women ≥ 18 years of age presenting with BI-RADS 4 breast masses identified on mammography or ultrasound were included in the study. Exclusion criteria comprised patients with a prior history of breast surgery or recurrent breast cancer, severe contrast allergies, contraindications to MRI, or those unwilling to participate in the study. Also, to minimize diagnostic bias, patients who had undergone a biopsy before the MRI examination were excluded from the study. Initially, 35 patients were recruited; after attrition, 31 masses from 29 patients were analyzed (**► Fig. 1**).

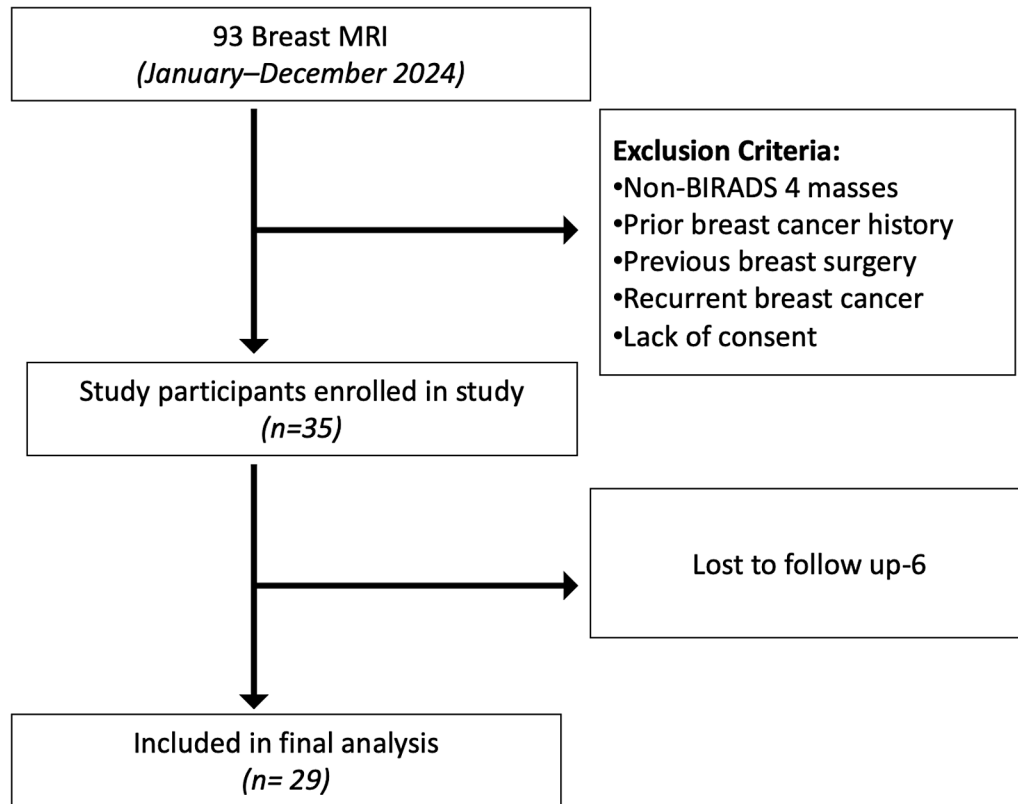


Fig. 1 Flow chart showing participant recruitment and attrition.

Study Protocol

All acquisitions were done on Siemens Magnetom Vida 3 Tesla MRI using a Tim Coil after obtaining informed consent. Patients were positioned in the prone position. Gadoteric acid 0.5 mmol/mL (0.1 mmol/kg DOTAREM) was injected through an intravenous cannula. MEDRAD Spectris Solaris EP, power injector, was started immediately after completion of the first phase in the time-resolved angiography with interleaved stochastic trajectories (TWIST) sequence to inject contrast at a rate of 2.5 mL/s. The ultrafast and full dynamic protocol was performed according to the pre-set sequences (→ **Table 1**).

The results from conventional MRI, standard DCE-MRI curves, and UF-MRI, including early kinetic parameters were independently evaluated by two radiologists with more than 10 years of experience in breast radiology. Both radiologists were blinded to each other's interpretations to prevent bias. The UF-MRI images were processed using the Syngo.via image analysis system (Siemens Healthineers). For lesion analysis, the region of interest was manually drawn over the most rapidly enhancing voxels within the breast masses, considered representative of the lesion. The kinetic parameters derived from these regions were then utilized to characterize the mass. For

Table 1 MRI protocol used for acquiring ultrafast and full dynamic protocols

Sequences	Plane	TR (ms)	TE (ms)	Slice thickness (mm)
STIR	Axial	4,100	68	3
T2 TSE	Axial	5,070	71	3
DWI	Axial	8,000	54	3
T1 FL3D Non-FS	Axial	5.1	2.37	1
T1 FL3D SPAIR	Axial	4.27	1.65	1
T1 VIBE TWIST DIXON	Axial	4.07	1.35	1.8
T1 dynamic postcontrast	Axial	4.27	1.65	1

Abbreviations: DWI, diffusion weighted imaging; FL3D, fast angle low shot 3-dimensional; FS, fat suppressed; SPAIR, spectrally adiabatic inversion recovery; STIR, short tau inversion recovery; TSE, turbo spin echo; TWIST, time-resolved angiography with interleaved stochastic trajectories; VIBE, volumetric interpolated breath-hold examination.

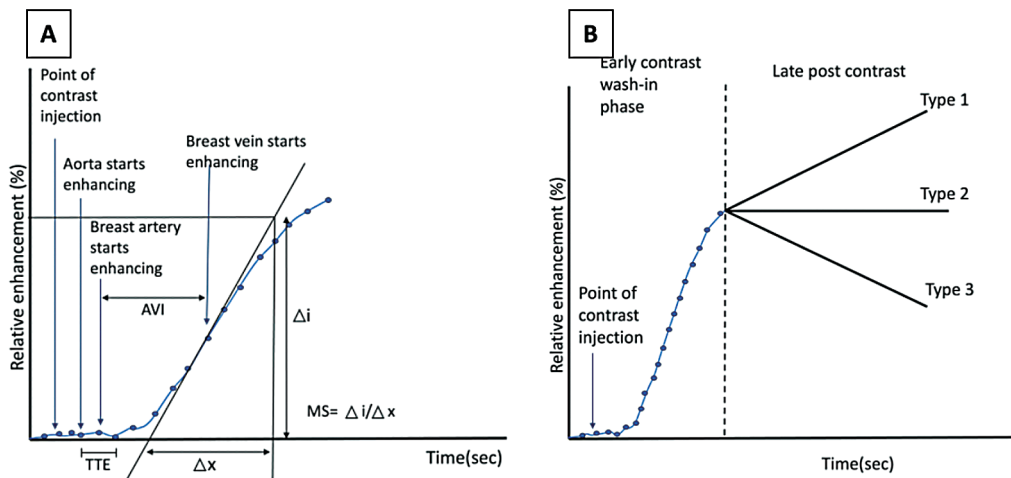


Fig. 2 Kinetic curves of UF-MRI and standard DCE-MRI. (A) Schematic diagram of relative enhancement versus time curves. The UF-MRI wash in kinetic curve with measurement of time to enhancement (TTE), maximum slope (MS), and arterial venous interval (AVI). The MS is measured by drawing a tangent at the steepest part of the wash-in curve; the TTE is measured as the time interval between enhancement of the aorta and that of the mass; and AVI is calculated as the time interval between the enhancement of the artery and vein. (B) Schematic diagram of relative enhancement versus time curves. The early phase represents the wash in kinetic curve of UF-MRI. The dynamic curves are classified as Type 1 (progressive enhancement), Type 2 (plateau), or Type 3 (washout). DCE-MRI, dynamic contrast-enhanced magnetic resonance imaging; UF-MRI, ultrafast magnetic resonance imaging.

statistical analysis, the median values from two independent radiologists were used.

For UF-MRI, specific kinetic parameters were used to analyze the wash-in curve in TWIST sequences (► Fig. 2A):

- TTE: the time interval between the enhancement of the aorta and the mass, with <12.96 s considered malignant and >12.96 s considered benign.¹⁷
- MS: the rate of enhancement, reflecting the steepness of the wash-in curve, with >13.3%/s considered malignant and <6.4%/s considered benign.¹⁶
- AVI: the time interval between the enhancement of the artery and the vein, with 8.14 to 11.84 s considered malignant and 12.94 to 19.61 s considered benign.¹⁸

The conventional DCE-MRI washout curves were also analyzed and categorized into three types: Type 1, Type 2, and Type 3 (► Fig. 2B). The kinetic data from the UF-MRI curves were compared with information derived from the standard DCE-MRI curves. All lesions were confirmed

Table 2 Number of the evaluated masses with their histopathological types

Malignant	(n = 16)
Invasive ductal carcinoma	13
Invasive lobular carcinoma	2
Ductal carcinoma in situ	1
Benign	(n = 15)
Fibroadenoma	10
Phyllodes	1
Sclerosing adenosis	2
Granulomatous mastitis	2

by core biopsy, with histopathology as the reference standard.

Statistical Analysis

The association between two categorical variables was examined using the Chi-squared test. If the estimated frequency in the contingency tables was less than 5 for more than 20% of the cells, Fisher’s exact test was employed instead. The receiver operator characteristic (ROC) curve was used for discriminating the power of TTE, MS, and AVI where histopathology was taken as the gold standard. Descriptive data were presented as means and standard deviations, as well as medians and interquartile ranges for continuous variables, and as percentages and frequencies for categorical variables.

Results

Demographics

The study included 31 masses from 29 patients. Among the patients included in the study, 61.3% were between 41 and 60 years of age, 29% were less than 40 years, and 9.7% were older than 60 years of age. The size of masses in our study ranged from 0.7 to 5.6 cm, with a mean size of 2.12 cm (standard deviation: 1.03) and a median of 2.3 cm. The BI-RADS classification on MRI was distributed as follows: BI-RADS 4C in 15 cases (48.4%), BI-RADS 4A in 11 cases (35.5%), and BI-RADS 4B in 5 cases (16.1%). Histopathological examination (HPE) revealed 16 malignant cases (51.6%) and 15 benign cases (48.4%). The most common malignant lesion was invasive ductal carcinoma not otherwise specified (13/16, 81%) followed by invasive lobular carcinoma (2/16, 12%), while the most common benign lesion was fibroadenoma (10/15, 67%; ► Table 2).

Table 3 Association between histopathology and full dynamic protocol of MRI including DCE-MRI

Findings	Characteristics	Histopathology		p-Value
		Malignant	Benign	
MRI: BI-RADS	3	0 (0.0%)	8 (53.3%)	< 0.001
	4	3 (18.8%)	6 (40.0%)	
	5	13 (81.2%)	1 (6.7%)	
MRI: standard DCE-MRI curve	Type 1	0 (0.0%)	6 (40.0%)	< 0.001
	Type 2	5 (31.2%)	8 (53.3%)	
	Type 3	11 (68.8%)	1 (6.7%)	
Shape	Round	0 (0.0%)	1 (6.7%)	0.002
	Oval	1 (6.2%)	8 (53.3%)	
	Irregular	15 (93.8%)	6 (40.0%)	
Margins	Circumscribed	0 (0.0%)	8 (53.3%)	0.002
	Irregular	9 (56.2%)	5 (33.3%)	
	Spiculated	7 (43.8%)	2 (13.3%)	
Internal enhancement characteristics	Homogenous	0 (0.0%)	3 (20.0%)	0.029
	Heterogenous	15 (93.8%)	10 (66.7%)	
	Rim enhancement	1 (6.2%)	0 (0.0%)	
	Dark internal septations	0 (0.0%)	2 (13.3%)	

Abbreviations: DCE-MRI, dynamic contrast-enhanced magnetic resonance imaging; MRI, magnetic resonance imaging.

Standard DCE-MRI Curve Evaluation

The washout MRI curves were evaluated and categorized into three types: Type 1, Type 2, and Type 3 (►Fig. 2B). All malignant cases exhibited either Type 2 or Type 3 curves. The majority of benign cases showed Type 1 (53.3%) or Type 2 (40%) curves, with one benign case presenting a Type 3 curve confirmed as granulomatous mastitis on histopathology. BI-RADS 5 ($n = 13$) and BI-RADS 4 ($n = 3$) were proven to be malignant on HPE. Additionally, all cases categorized as BI-RADS 3 were confirmed to be benign through histopathological correlation (►Table 3).

UF-MRI Evaluation

There was a statistically significant difference among the benign and malignant masses in the distribution of TTE

($\chi^2 = 20.884$, $p < 0.001$), AVI ($\chi^2 = 23.881$, $p < 0.001$), and MS ($\chi^2 = 9.597$, $p = 0.010$; ►Table 4). TTE and AVI demonstrated strong associations with the histopathology results, with bias-corrected Cramer's V values of 0.81 and 0.87, respectively. In contrast, MS showed a moderate association, with a bias-corrected Cramer's V value of 0.50. TTE and AVI demonstrated perfect sensitivity, correctly identifying all 16 malignant cases confirmed by histopathology. In comparison, MS correctly classified 9 out of 16 malignant lesions, misclassified 2 as benign, and categorized 5 as equivocal. Among benign lesions, TTE yielded three false positives, while AVI produced two, with all remaining cases accurately classified. Conversely, MS misclassified 3 out of 15 benign lesions as malignant, correctly identified 10, and labeled 2 as equivocal. These results suggest that TTE

Table 4 Table showing an association between histopathology and UF-MRI parameters

Parameters	Values	Histopathology		p-Value
		Malignant	Benign	
UF-MRI: TTE (s)	< 12.96	16 (100.0%)	3 (20.0%)	< 0.001
	> 12.96	0 (0.0%)	12 (80.0%)	
UF-MRI: AVI (s)	8.14–11.84	16 (100.0%)	2 (13.3%)	< 0.001
	12.94–19.61	0 (0.0%)	13 (86.7%)	
UF-MRI: MS (%/s)	> 13.3	9 (56.2%)	3 (20.0%)	0.010
	< 6.4	2 (12.5%)	10 (66.7%)	
	6.4–13.3	5 (31.2%)	2 (13.3%)	

Abbreviations: AVI, arterial venous interval; MS, maximum slope; TTE, time to enhancement; UF-MRI, ultrafast magnetic resonance imaging.

and AVI offer superior diagnostic reliability in differentiating malignant from benign lesions, whereas MS demonstrates moderate accuracy.

Comparative Analysis of the Morphology of Mass and the UF-MRI Parameters

Irregular-shaped masses had the highest proportion of TTE <12.96 seconds and AVI values between 8.14 and 11.84. Similarly, masses with spiculated margins predominantly exhibited TTE <12.96 seconds and AVI values within the same range. In contrast, masses with circumscribed margins were most commonly associated with TTE >12.96 seconds and AVI values ranging from 12.94 to 19.61. MS showed little to no association with the shape or margin of the masses.

Comparative Analysis of Standard DCE-MRI with UF-MRI

The UF-MRI parameters TTE and AVI exhibited a significant correlation with standard MRI enhancement curve types. Notably, lesions classified as Type 3 on the standard MRI curve showed the highest proportion of TTE values <12.96 seconds and AVI values ranging from 8.14 to 11.84, indicating a strong association between early contrast kinetics and malignancy.

TTE, AVI, and the standard MRI curve were all found to be 100% sensitive in detecting malignant pathology. MS showed a sensitivity of 87.5%. The standard DCE-MRI curves had a significantly lower specificity at 40%, whereas AVI demonstrated the highest specificity at 86.7%, TTE at 80%, followed by MS at 66.7%.

Among all parameters, AVI showed the highest overall diagnostic performance, surpassing TTE and MS in terms of diagnostic accuracy, sensitivity, specificity, PPV, and negative predictive value (NPV). The combined accuracy of TTE + AVI + MS was 93.5%. In contrast, the standard DCE-MRI kinetic curves had a lower diagnostic accuracy of 71% (► Table 5).

As per logistic regression analysis, the area under the ROC curve (AUROC) for the combined UF-MRI parameters (TTE + AVI + MS) in predicting malignancy based on histopathology was 0.969 (95% confidence interval [CI]: 0.913–1.0), indicating excellent diagnostic performance. This result was statistically significant ($p < 0.001$). UF-MRI showed high sensitivity and specificity of 100 and 87%, respectively (► Fig. 3).

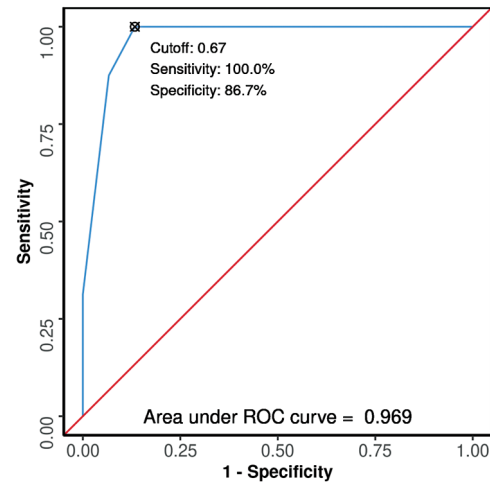


Fig. 3 ROC curve analysis showing diagnostic performance of ultrafast MRI (TTE + AVI + MS). AVI, arterial venous interval; MRI, magnetic resonance imaging; MS, maximum slope; ROC, receiver operating curve; TTE, time to enhancement.

Discussion

Breast malignancy remains one of the leading causes of cancer-related deaths among women worldwide as well as in the Indian population.^{1,19} Alarming, an increasing number of younger women are being diagnosed. Younger patients often have denser breast tissue, which significantly reduces the sensitivity of conventional imaging modalities such as mammography and ultrasonography.²⁰ Ultrasonography, although a valuable adjunct, is highly operator-dependent, with variability in diagnostic accuracy. These challenges are especially pronounced in cases involving multifocal and multicentric masses, where both modalities struggle to provide a comprehensive assessment of disease extent.

The advent of breast MRI has revolutionized breast cancer imaging by offering unparalleled sensitivity and the ability to detect high-grade and invasive tumors at earlier stages, improving interval cancer detection and patient survival.^{4–8} Expanding the adoption of MRI, especially for younger women and those with dense breasts, is essential for improving early detection rates and enhancing survival

Table 5 Comparative analysis of UF-MRI parameters and standard DCE-MRI

Variable	Sensitivity	Specificity	PPV	NPV	Diagnostic accuracy
UF-MRI: TTE	100.0% (79–100)	80.0% (52–96)	84.2% (60–97)	100.0% (74–100)	90.3% (74–98)
UF-MRI: AVI	100.0% (79–100)	86.7% (60–98)	88.9% (65–99)	100.0% (75–100)	93.5% (79–99)
UF-MRI: MS	87.5% (62–98)	66.7% (38–88)	73.7% (49–91)	83.3% (52–98)	77.4% (59–90)
MRI: standard MRI curve	100.0% (79–100)	40.0% (16–68)	64.0% (43–82)	100.0% (54–100)	71.0% (52–86)
UF-MRI: (TTE + AVI + MS)	100.0% (79–100)	86.7% (60–98)	88.9% (65–99)	100.0% (75–100)	93.5% (79–99)

Abbreviations: AVI, arterial venous interval; DCE-MRI, dynamic contrast-enhanced magnetic resonance imaging; PPV, positive predictive value; MRI, magnetic resonance imaging; MS, maximum slope; NPV, negative predictive value; TTE, time to enhancement; UF-MRI, ultrafast magnetic resonance imaging.

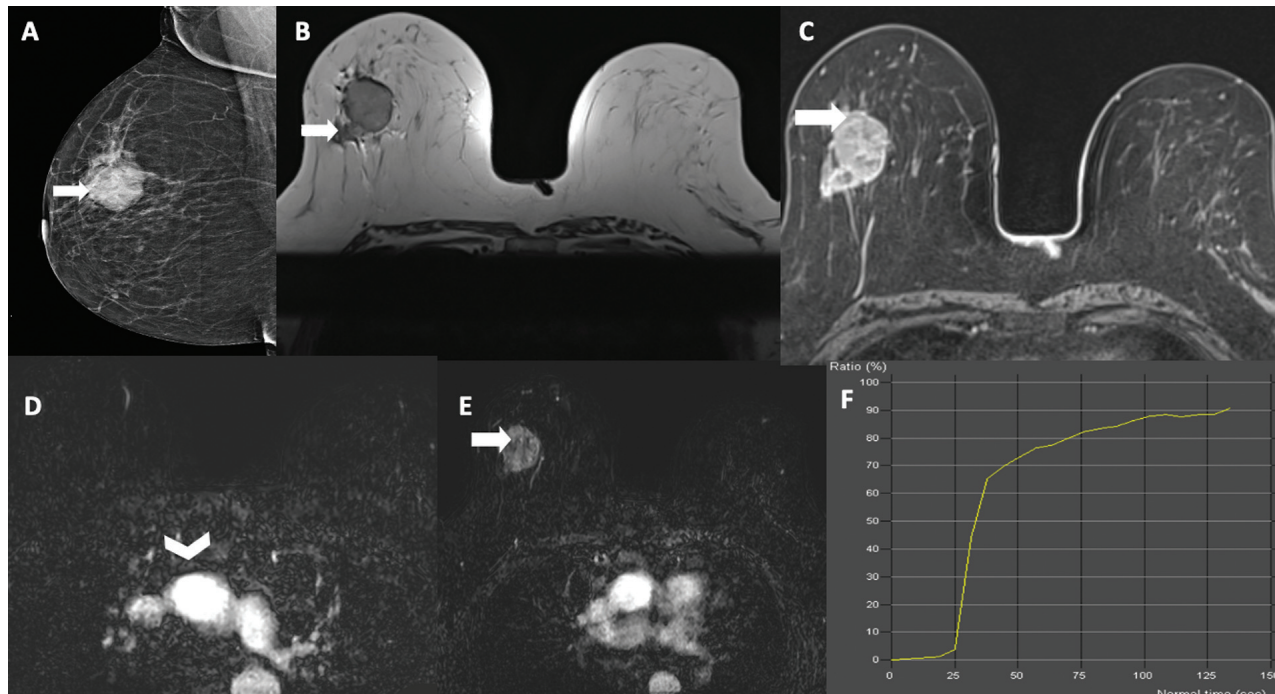


Fig. 4 A 68-year-old female presented with right nipple discharge for 5 months without a palpable lump. (A) The right mediolateral oblique (MLO) mammography view shows a high-density, irregular mass in the upper breast (white arrow). (B and C) Axial T2-weighted (4B) and precontrast T1 SPAIR (4C) images reveal an irregular mass with spiculated margins at the 11 o'clock position (white arrow). (D and E) Postcontrast (VIBE TWIST) axial subtracted images demonstrate contrast enhancement of the aorta (arrowhead) in phase 4 (4D), with immediate enhancement of the right breast mass (white arrow) in subsequent phase 5 (4E), with a TTE of 6.32 seconds. Minimal background parenchymal enhancement is noted. (F) Kinetic curve (time on the x-axis, relative enhancement on the y-axis) shows rapid early enhancement of the mass. Histopathology confirmed invasive ductal carcinoma not otherwise specified. TWIST, time-resolved angiography with interleaved stochastic trajectories; VIBE, volumetric interpolated breath-hold examination.

outcomes in breast cancer patients. However, widespread adoption in India remains constrained by high costs, limited availability, longer acquisition times, and lower specificity.

Kinetic information plays a crucial role in distinguishing benign from malignant breast lesions on MRI. However, standard kinetic assessment faces challenges such as misregistration artifacts in subtracted images caused by long acquisition times, which can compromise image quality and diagnostic accuracy. UF-MRI offers a promising solution by significantly reducing acquisition times while maintaining diagnostic accuracy making MRI a more practical and accessible tool, particularly in resource-constrained settings.

The concept of abbreviated MRI was put forward by Kuhl et al¹¹ in 2014 which decreased the magnet time to around 3 minutes by acquiring only the precontrast and first post-contrast images. It showed a high NPV of 99.8%. However, it lacked kinetic information. Although multiple-phase images can be obtained postcontrast injection, the most clinically relevant information is captured during the early phase. In later phases, BPE increases, potentially obscuring true lesions and reducing the usefulness of delayed-phase images. UF-MRI addressed this limitation by incorporating dynamic information on wash-in-contrast kinetics, eliminating reliance on the conventional washout curve. This required achieving high temporal resolution, allowing repeated ac-

quisition of the same image set within seconds without significantly compromising spatial resolution. Innovations in acquisition techniques, such as view sharing, compressed sensing, and parallel imaging, were instrumental in bringing this breakthrough, making UF-MRI a valuable tool in modern breast imaging.^{12–15,20}

UF-MRI is particularly effective in detecting hypervascularity, a hallmark of most malignant tumors, which distinguishes them from benign lesions. Mann et al aptly described this phenomenon, noting that such tumors “stand out like a light bulb” against the background breast parenchyma.¹⁶ One of the key advantages of UF-MRI is its ability to bring forth malignant masses before the setting in of BPE, making it especially beneficial for young women at high risk for breast cancer, who often exhibit moderate to marked BPE (►Fig. 4).²¹ Early wash-in kinetic parameters such as MS, TTE, and AVI have demonstrated high accuracy in differentiating malignant from benign lesions.^{17,18}

We evaluated 29 patients with 31 BI-RADS 4 breast masses using the UF-MRI protocol, followed by the full dynamic protocol, to compare the sensitivity, specificity, and diagnostic accuracy of the kinetic parameters. Our findings revealed that TTE and AVI demonstrated comparable sensitivity (100%) and specificity (80% and 86.7%), with AVI showing a slight advantage in both specificity and overall diagnostic accuracy. MS while exhibiting reasonable sensitivity (87.5%) and specificity (66.7%)

showed moderate performance relative to TTE and AVI. The combined diagnostic performance of TTE, AVI, and MS was also assessed, yielding an AUROC of 0.969 (95% CI: 0.913–1), indicating statistically significant and excellent diagnostic performance. However, the combined performance did not significantly surpass the individual performance of AVI.

Our findings align with a recent meta-analysis by Amitai et al,²² which concluded that the combination of multiple kinetic parameters did not substantially improve the differentiation between benign and malignant masses. This observation was attributed to the shared principles of contrast kinetics, such as capillary leakage and arteriovenous shunting, underlying these parameters. Consequently, our study supports the notion that evaluating multiple kinetic parameters rooted in the same physiological mechanisms may be redundant and unnecessary. This highlights the potential for a more streamlined approach in the interpretation of UF-MRI findings.

Our study revealed a significant association between lesion shape and UF-MRI parameters such as TTE and AVI. Irregularly shaped and spiculated masses predominantly exhibited shorter TTE (<12.96 s) and AVI (8.14–11.84), char-

acteristics associated with malignancy. Conversely, circumscribed margins were more likely to exhibit longer TTE and AVI values, indicative of benignity (►Fig. 5). MS, however, showed minimal association with either shape or margins and proved to be inferior in this aspect.

The Type 3 curve on standard DCE-MRI demonstrated a strong association with shorter TTE (<12.96 s) and AVI (8.14–11.84), consistent with the kinetic profiles of malignant lesions. Conversely, the Type 1 curve was consistently linked to longer TTE (>12.96 s) and AVI (12.94–19.61), reflecting the kinetics typically seen in benign lesions. The Type 2 curve, however, exhibited significant overlap between benign and malignant lesions, introducing diagnostic ambiguity.

In a study by Mus et al., utilizing Siemens Magnetom Skyra or Trio 3T MRI scanners, TWIST sequences were used for UF-MRI acquisition. After evaluating TTE in 164 lesions, they revealed a sensitivity of 93.9 and 90.0% and specificity of 79.2 and 77.2% respectively, for readers 1 and 2. A cut-off of 12.96 seconds was used, where masses with TTE <12.96 were considered malignant. At a similar TTE cut-off of 12.96, our study acquisitions on Siemens Magnetom Vida

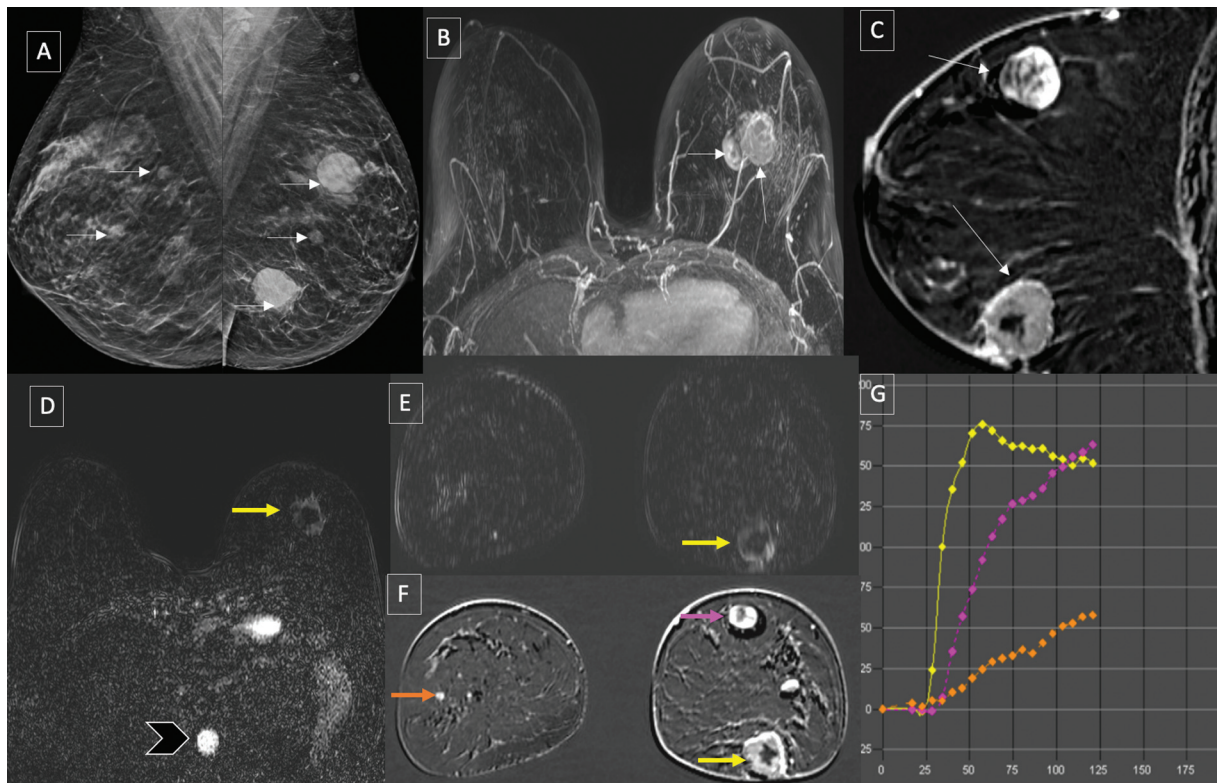


Fig. 5 A 37-year-old female presented with a left breast lump persisting for 7 months. (A) Bilateral mammogram, mediolateral oblique (MLO) views, reveals multiple masses of varying sizes in both breasts (thin white arrows). (B) Axial maximum intensity projection (MIP) image from phase 20 of VIBE TWIST demonstrates two distinct masses in the left breast (thin arrows) in the upper and lower halves of the left breast. (C) Sagittal postcontrast image (one minute) shows heterogeneous enhancement of the masses (thin arrows) at the 6 o'clock and 12 o'clock positions in the left breast. (D, E, and F) UF-MRI images depict early differential enhancement of the mass at the 6 o'clock in the left breast, compared with the rest of the masses in bilateral breasts. (G) Kinetic curves depict contrast enhancement patterns of the left 6 o'clock mass (yellow) and 12 o'clock mass (pink), as well as of the right breast mass (orange). The 6 o'clock mass exhibits rapid enhancement with a steep slope, suggestive of malignancy, while the 12 o'clock and right breast masses show slower enhancement with shallower slopes, indicative of benign pathology. Histopathology confirmed the 6 o'clock mass as invasive ductal carcinoma, while the other masses were fibroadenomas. TWIST, time-resolved angiography with interleaved stochastic trajectories; UF-MRI, ultrafast magnetic resonance imaging; VIBE, volumetric interpolated breath-hold examination.

3T revealed a sensitivity of 100% and specificity of 80%. Mann et al reported that using a cut-off of 13.3% for the MS achieved a specificity of 85% and a sensitivity of 65%. When all masses with an MS above 6.4% were classified as malignant, sensitivity improved, but specificity decreased to 67%.¹⁶

In our study, we categorized MS values into three ranges: <6.4% (benign), 6.4 to 13.3% (equivocal/intermediate risk), and >13.3% (malignant). Using these thresholds, we observed that MS achieved a sensitivity of 87.5%, a specificity of 66.7%, and an overall diagnostic accuracy of 77.4%. These findings highlight the utility of MS as a diagnostic parameter while also reflecting the trade-off between sensitivity and specificity at different cut-off values.

Honda et al compared the kinetic parameters of UF-MRI with the conventional MRI washout curve. They found AVI to have a sensitivity, specificity, and diagnostic accuracy of 88, 39, and 73%, respectively. Also, the conventional MRI washout curve was found to have a sensitivity, specificity, and diagnostic accuracy of 90, 48, and 77%, respectively. In our study, AVI outperformed these results, achieving a sensitivity of 100%, a specificity of 86.7%, and a diagnostic accuracy of 93.5%. Conversely, the conventional MRI washout curve in our cohort demonstrated a sensitivity of 100%, a specificity of 40%, and a diagnostic accuracy of 71%. These findings highlight the superior diagnostic performance of AVI in UF-MRI compared with conventional MRI washout curves, particularly in specificity and overall accuracy.

Our study identified hypervascular benign lesions like granulomatous mastitis and sclerosing adenosis as a key

source of false positives (→ Fig. 6). This emphasizes the need for caution in interpreting UF-MRI findings, especially in young women or premenopausal patients with dense breast tissue, where benign hypervascular lesions are more common.

The primary limitation of this study is its small sample size, which may affect the robustness of the findings. Additionally, the focus on BI-RADS 4 lesions may have led to an incomplete assessment of the full spectrum of imaging characteristics across different benign and malignant histopathological subtypes. However, analysis of BI-RADS 4 lesions is of utmost importance as a decision for these lesions is often evasive, as they have a wide possibility of being malignant, ranging from as low as 2% to as high as 95%. Further large-scale, multicenter studies are needed to validate our results and establish standardized UF-MRI thresholds for clinical use. Efforts should focus on developing uniform UF-MRI protocols, including fixed injection rates, scan timings, and parameter thresholds to improve inter-institutional reproducibility. Radiomic analysis of UF-MRI data could uncover additional tumor features not discernible visually. Integration with artificial intelligence algorithms may enable automated lesion classification and risk stratification. Research into simplified acquisition techniques and cost-reduction strategies, such as compressed sensing, could make UF-MRI a more viable option in resource-limited settings. Innovations in acquisition techniques and cost-reduction strategies will be critical to increasing accessibility and standardizing UF-MRI globally.

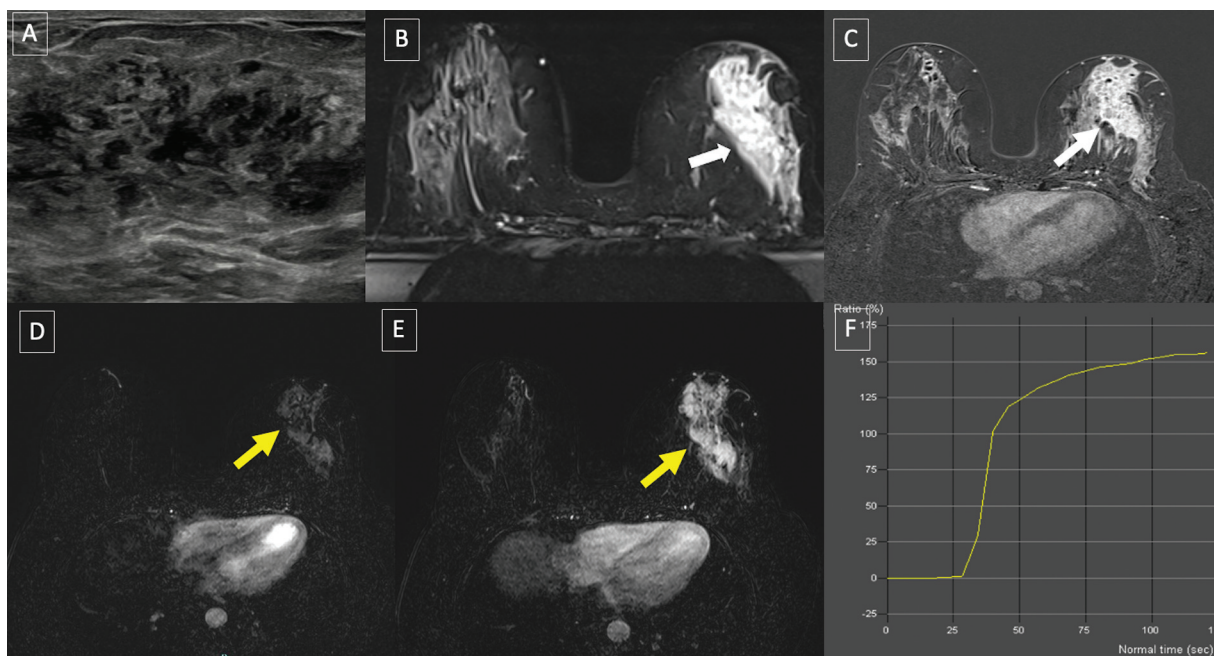


Fig. 6 A 29-year-old female presented with a left breast lump. (A) Ultrasonogram reveals an irregular hypoechoic mass (white arrow) in the lower central breast. (B): Axial STIR image demonstrates an irregular mass at the 5 to 7 o'clock position (white arrow). (C) Postcontrast axial VIBE TWIST-subtracted maximum intensity projection (MIP) image shows an irregular enhancing mass at the 5 to 7 o'clock position (white arrow). (D and E) Axial postcontrast subtracted T1 SPAIR image reveals heterogeneous enhancement in masses at the 5 to 7 o'clock (white arrow) and 12 o'clock positions (arrowhead). (F) Kinetic curve analysis of UF-MRI shows a rapid upslope with a high maximum slope (MS) of 19.6 and TTE of 5.8 seconds, favoring malignant etiology. However, histopathology confirmed granulomatous mastitis. TWIST, time-resolved angiography with interleaved stochastic trajectories; UF-MRI, ultrafast magnetic resonance imaging; VIBE, volumetric interpolated breath-hold examination.

Conclusion

UF-MRI provides a rapid and precise method for differentiating benign from malignant BI-RADS 4 lesions, with TTE and AVI standing out as highly reliable diagnostic markers. Combining these kinetic parameters with morphological features like shape and margins significantly enhances diagnostic accuracy, reducing unnecessary biopsies and facilitating precise preoperative planning. The findings of this study highlight the potential of UF-MRI as a highly specific and sensitive time-saving tool. Future research with a larger study population should focus on standardizing UF-MRI protocols and integrating complementary imaging techniques to improve specificity and ensure broader clinical applicability.

Conflict of Interest

None declared.

References

- Siegel RL, Miller KD, Jemal A. Cancer statistics, 2020. *CA Cancer J Clin* 2020;70(01):7–30
- Tabár L, Vitak B, Chen TH, et al. Swedish two-county trial: impact of mammographic screening on breast cancer mortality during 3 decades. *Radiology* 2011;260(03):658–663
- Sung JS, Stampler S, Brooks J, et al. Breast cancers detected at screening MR imaging and mammography in patients at high risk: method of detection reflects tumor histopathologic results. *Radiology* 2016;280(03):716–722
- Kuhl CK, Strobel K, Bieling H, Leutner C, Schild HH, Schrading S. Supplemental breast MR imaging screening of women with average risk of breast cancer. *Radiology* 2017;283(02):361–370
- Riedl CC, Luft N, Bernhart C, et al. Triple-modality screening trial for familial breast cancer underlines the importance of magnetic resonance imaging and questions the role of mammography and ultrasound regardless of patient mutation status, age, and breast density. *J Clin Oncol* 2015;33(10):1128–1135
- Kuhl C, Weigel S, Schrading S, et al. Prospective multicenter cohort study to refine management recommendations for women at elevated familial risk of breast cancer: the EVA trial. *J Clin Oncol* 2010;28(09):1450–1457
- Vreemann S, Gubern-Mérida A, Schlooz-Vries MS, et al. Influence of risk category and screening round on the performance of an MR imaging and mammography screening program in carriers of the BRCA mutation and other women at increased risk. *Radiology* 2018;286(02):443–451
- Luiten JD, Voogd AC, Luiten EJT, Duijm LEM. Trends in incidence and tumour grade in screen-detected ductal carcinoma in situ and invasive breast cancer. *Breast Cancer Res Treat* 2017;166(01):307–314
- Sardanelli F, Podo F. Breast MR imaging in women at high-risk of breast cancer. Is something changing in early breast cancer detection? *Eur Radiol* 2007;17(04):873–887
- Podo F, Santoro F, Di Leo G, et al. Triple-negative versus non-triple-negative breast cancers in high-risk women: phenotype features and survival from the HIB CRIT-1 MRI-including screening study. *Clin Cancer Res* 2016;22(04):895–904
- Kuhl CK, Schrading S, Strobel K, Schild HH, Hilgers RD, Bieling HB. Abbreviated breast magnetic resonance imaging (MRI): first postcontrast subtracted images and maximum-intensity projection—a novel approach to breast cancer screening with MRI. *J Clin Oncol* 2014;32(22):2304–2310
- Saranathan M, Rettmann DW, Hargreaves BA, Clarke SE, Vasana-wala SS. Differential Subsampling with Cartesian Ordering (DISCO): a high spatio-temporal resolution Dixon imaging sequence for multiphasic contrast enhanced abdominal imaging. *J Magn Reson Imaging* 2012;35(06):1484–1492
- Lustig M, Donoho D, Pauly JM. Sparse MRI: The application of compressed sensing for rapid MR imaging. *Magn Reson Med* 2007;58(06):1182–1195
- Sagawa H, Kataoka M, Kanao S, et al. Impact of the number of iterations in compressed sensing reconstruction on ultrafast dynamic contrast-enhanced breast MR imaging. *Magn Reson Med Sci* 2019;18(03):200–207
- Jaspan ON, Fleysler R, Lipton ML. Compressed sensing MRI: a review of the clinical literature. *Br J Radiol* 2015;88(1056):20150487
- Mann RM, Mus RD, van Zelst J, Geppert C, Karssemeijer N, Platel B. A novel approach to contrast-enhanced breast magnetic resonance imaging for screening: high-resolution ultrafast dynamic imaging. *Invest Radiol* 2014;49(09):579–585
- Mus RD, Borelli C, Bult P, et al. Time to enhancement derived from ultrafast breast MRI as a novel parameter to discriminate benign from malignant breast lesions. *Eur J Radiol* 2017;89:90–96
- Onishi N, Kataoka M, Kanao S, et al. Ultrafast dynamic contrast-enhanced mri of the breast using compressed sensing: breast cancer diagnosis based on separate visualization of breast arteries and veins. *J Magn Reson Imaging* 2018;47(01):97–104
- Malvia S, Bagadi SA, Dubey US, Saxena S. Epidemiology of breast cancer in Indian women. *Asia Pac J Clin Oncol* 2017;13(04):289–295
- Berg WA, Blume JD, Cormack JB, et al; ACRIN 6666 Investigators. Combined screening with ultrasound and mammography vs mammography alone in women at elevated risk of breast cancer. *JAMA* 2008;299(18):2151–2163
- Honda M, Kataoka M, Iima M, et al. Background parenchymal enhancement and its effect on lesion detectability in ultrafast dynamic contrast-enhanced MRI. *Eur J Radiol* 2020;129:108984
- Amitai Y, Freitas VAR, Golan O, et al. The diagnostic performance of ultrafast MRI to differentiate benign from malignant breast lesions: a systematic review and meta-analysis. *Eur Radiol* 2024;34(10):6285–6295